Buoyancy-driven convection in a horizontal porous layer saturated by a power-law fluid: The effect of an open boundary

Michele Celli, Andrea Natale Impiombato, Antonio Barletta, *Buoyancy-driven convection in a horizontal porous layer saturated by a power-law fluid: The effect of an open boundary*, International Journal of Thermal Sciences, Volume 152, 2020, 106302

ISSN 1290-0729

Buoyancy–driven convection in a horizontal porous layer saturated by a power–law fluid: the effect of an open boundary

Michele Celli[a,*], Andrea Natale Impiombato[a], Antonio Barletta[a]

[a] *Alma Mater Studiorum Università di Bologna, Department of Industrial Engineering, Viale Risorgimento 2, 40136 Bologna, Italy*

Abstract

An infinitely wide horizontal porous layer saturated by a power–law fluid is heated from below by an imposed heat flux. The basic stationary state is characterised by a horizontal throughflow and a constant temperature gradient along the vertical direction. A linear stability analysis is performed by employing the method of normal modes. The eigenvalue problem obtained is solved by employing two different approaches: a hybrid analytical/numerical technique and a fully numerical technique. The critical values defining the threshold configurations for the onset of thermal convection are presented. These threshold values display a non monotonic dependence on the basic flow rate while they are monotonically increasing functions of the power–law index.

Keywords: Thermal convection, Porous medium, Power–law fluid, Linear stability analysis, Open boundary

1. Introduction

The onset of thermal convection in fluid saturated porous media is a topic that draws attention from theoretical research areas, such as applied mathematics, and from engineering oriented research areas, such as the analysis of geothermal resources and the design of repositories for nuclear debris, [1].

A cornerstone study within this research topic is the problem originally investigated by Horton and Rogers [2] and Lapwood [3] (HRL). The HRL problem is the analogue, for fluid saturated porous media, of the Rayleigh–Bénard problem. Since Darcy's law is employed to model the momentum transport, the HRL problem is also called the Darcy–Bénard problem. The threshold value of the governing parameter, *i.e.* the Darcy–Rayleigh number, evaluated by the linear stability analysis is $4\,\pi^2$. This value does not change when a basic throughflow is added to the stationary basic state. The pioneering study regarding this configuration was presented by Prats [4]. In both the Darcy–Bénard problem and in the Prats problem, the porous medium is saturated by a Newtonian fluid. The literature relative to convection in porous media, in fact, mainly deals with Newtonian fluids [1]. Nonetheless, the non–Newtonian fluids are extremely common and they have widespread applications: from food industry processes to bioengineering and oil extraction engineering [5]. A review of heat transfer in porous media saturated by non–Newtonian fluids is can be found in Shenoy [6]. Some further work on the stability analysis relative to non–Newtonian fluids saturating a porous layer has been carried out by Barletta and Nield [7], by Celli et al. [8]. Further papers relative to buoyant flows of power–law fluids in porous media are by Nakayama and Shenoy [9] and by Shenoy [10].

This paper presents the linear stability analysis of a modified Prats problem where a power–law fluid saturates the horizontal porous layer. Other differences, as compared to the Prats problem, are the assumptions of an open upper boundary and of a uniform heat flux at the lower boundary. To the best of the authors knowledge, this is the first study regarding the stability analysis of the throughflow of a power–law

*Corresponding author. Tel.: (+39) 051 2093285.
Email address: michele.celli3@unibo.it (Michele Celli)

fluid saturating a porous layer with a permeable boundary. This configuration can be relevant for the investigation of heat and mass transfer in underground fluid reservoirs where hydrocarbons may be modelled as non–Newtonian fluids. A well–known effect of assuming open boundaries is the lower value of the critical Darcy–Rayleigh number with respect to that for impermeable boundaries [1]. In other words, the effect of open boundaries is a destabilisation of the basic fluid flow. The aim of the present analysis is investigating the effect of an open boundary on the onset of thermal convection when a power–law fluid saturated porous medium is involved.

2. Mathematical model

A horizontal porous layer saturated by a power–law fluid is heated from below by a constant heat flux. The layer is infinitely wide in the x and z directions and confined in the y direction by an impermeable lower boundary and an isothermal open upper boundary. A sketch of the porous layer is presented in Fig. 1. For a power–law fluid, the shear stress, τ, depends nonlinearly on the shear rate, $\dot{\gamma}$,

$$\tau = \eta\,\dot{\gamma}^n, \tag{1}$$

where η is the consistency index measured in $\mathrm{Pa\,s}^n$, and n is the power–law index. Equation (1) yields the following definition of apparent viscosity $\tilde{\mu}$:

$$\tilde{\mu} = \eta\,\dot{\gamma}^{n-1}. \tag{2}$$

For a power–law fluid, a modified Darcy's law has been formulated [11, 12] which, in a dimensionless form, can be written as

$$\boldsymbol{\nabla} \times \left(|\mathbf{u}|^{n-1}\mathbf{u}\right) = R\,\boldsymbol{\nabla} \times (T\mathbf{e}_y)\,, \tag{3}$$

where the buoyancy force is modelled by means of the Oberbeck–Boussinesq approximation, $\mathbf{x} = (x, y, z)$ is the Cartesian position vector, $\mathbf{u} = (u, v, w)$ is the filtration velocity vector, R is the modified Darcy–Rayleigh number, T is the temperature and $\mathbf{e}_y$ is the unit vector in the y direction. The curl operator is applied to the momentum balance equation to encompass the contribution of the pressure gradient.
The energy balance equation employed to model the heat transfer is the convection/conduction equation where no source/sink term is considered. Thus, the dimensionless governing equations are given by

$$\begin{aligned}
&\boldsymbol{\nabla}\cdot\mathbf{u} = 0,\\
&\boldsymbol{\nabla} \times \left(|\mathbf{u}|^{n-1}\mathbf{u}\right) = R\,\boldsymbol{\nabla} \times (T\mathbf{e}_y)\,,\\
&\frac{\partial T}{\partial t} + \mathbf{u}\cdot\boldsymbol{\nabla}T = \nabla^2 T,\\
&y = 0: \qquad v = 0, \quad \frac{\partial T}{\partial y} = -1,\\
&y = 1: \qquad \frac{\partial v}{\partial y} = 0, \quad T = 0.
\end{aligned} \tag{4}$$

The dimensionless formulation presented in Eq. (4) relies on the following scaling:

$$\frac{\mathbf{x}}{H} \to \mathbf{x}, \quad \frac{\chi}{\sigma H^2}t \to t, \quad \frac{H}{\chi}\mathbf{u} \to \mathbf{u}, \quad \frac{T - T_0}{\Delta T} \to T, \tag{5}$$

where $\Delta T = q_0\,H/k_{eff}$, H is the porous layer height, σ is the heat capacity ratio, χ is the ratio between the effective thermal conductivity k_{eff} of the fluid saturated porous medium and the heat capacity of the fluid, T_0 is the temperature of the upper boundary while q_0 is the heat flux prescribed at the lower boundary. More precisely, σ, k_{eff} and χ, are defined as

$$\sigma = \frac{\varphi\,\rho_f c_f + (1-\varphi)\,\rho_s\,c_s}{\rho_f\,c_f}, \quad k_{eff} = \varphi\,k_f + (1-\varphi)\,k_s, \quad \chi = \frac{k_{eff}}{\rho_f\,c_f}. \tag{6}$$

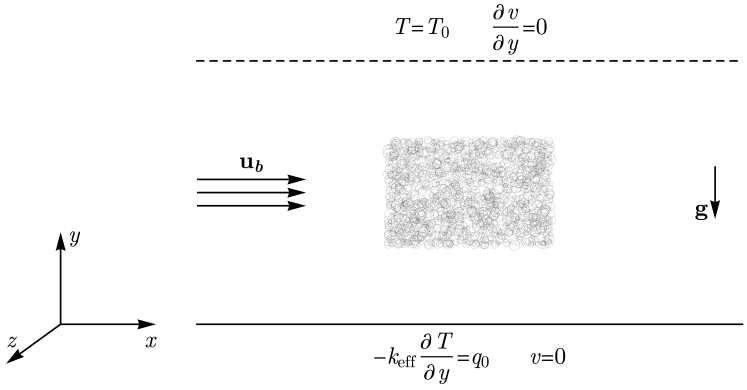

Figure 1: A sketch of the horizontal porous layer

In Eq. (4), the modified Darcy–Rayleigh number is given by

$$R = \frac{\rho_f \, g \, \beta \, \Delta T \, K \, H^n}{\eta \, \chi^n}, \quad \sigma = \frac{\varphi \, \rho_f c_f + (1-\varphi) \, \rho_s \, c_s}{\rho_f \, c_f}, \quad k_{eff} = \varphi \, k_f + (1-\varphi) \, k_s, \quad \chi = \frac{k_{eff}}{\rho_f \, c_f}. \tag{7}$$

In Eqs. (6) and (7), ρ_f is the fluid density evaluated at the reference temperature T_0, g is the modulus of the gravitational acceleration vector $\mathbf{g}$ (see Fig. 1), β is the thermal expansion coefficient relative to the fluid, K is the generalised permeability of the porous medium measured in m^{n+1}, φ is the porosity, c_f is the specific heat capacity of the fluid, c_s is the specific heat capacity of the porous medium, ρ_s is the density of the porous medium, k_f is the thermal conductivity of the fluid and k_s is the thermal conductivity of the porous medium.

2.1. Basic state

The system of partial differential equations defined by (4) admits a stationary solution characterised by a uniform velocity profile directed along the x axis, namely

$$\mathbf{u}_b = (Pe, 0, 0), \tag{8}$$

where the subscript b denotes the quantities relative to the basic state and Pe is the Péclet number. Consistently with Eq. (8), the temperature profile depends only on y direction. From Eq. (4), one obtains the basic temperature profile, namely

$$T_b = 1 - y. \tag{9}$$

3. Linear stability analysis

With the aim of investigating the linear stability of the system described in Section 2, the basic state described in Eqs. (8) and (9) is perturbed by small amplitude disturbances. The amplitude of such disturbances changes with time and, depending on the governing parameters, it may decay (yielding a stable basic state) or it may grow (producing a buoyancy–induced cellular flow). In the following analysis, the threshold between decaying and growing disturbances defines the so–called neutral stability condition. Thus, the velocity and temperature fields are written as

$$\mathbf{u} = \mathbf{u}_b + \varepsilon \mathbf{U}, \qquad T = T_b + \varepsilon \Theta, \tag{10}$$

where $\varepsilon \ll 1$. By substituting Eq. (10) into Eq. (4) and by neglecting terms $O(\varepsilon^2)$ or higher, one obtains the linearised governing equations describing the dynamics of disturbances,

$$\begin{aligned}
&\frac{\partial U}{\partial x}+\frac{\partial V}{\partial y}+\frac{\partial W}{\partial z}=0,\\
&\frac{\partial V}{\partial z}-\frac{\partial W}{\partial y}=\frac{R}{Pe^{n-1}}\frac{\partial \Theta}{\partial z},\\
&n\frac{\partial U}{\partial z}-\frac{\partial W}{\partial x}=0,\\
&n\frac{\partial U}{\partial y}-\frac{\partial V}{\partial x}=-\frac{R}{Pe^{n-1}}\frac{\partial \Theta}{\partial x},\\
&\frac{\partial \Theta}{\partial t}+Pe\frac{\partial \Theta}{\partial x}-V=\nabla^2\Theta,\\
&y=0: \qquad V=0, \quad \frac{\partial \Theta}{\partial y}=-1,\\
&y=1: \qquad \frac{\partial V}{\partial y}=0, \quad \Theta=0.
\end{aligned} \tag{11}$$

By manipulating Eq. (11), one may obtain a simplified system of equations which contains only the two fields (V, Θ), namely

$$\begin{aligned}
&\frac{\partial^2 V}{\partial x^2}+n\frac{\partial^2 V}{\partial y^2}+n\frac{\partial^2 V}{\partial z^2}=\frac{R}{Pe^{n-1}}\left(\frac{\partial^2 \Theta}{\partial x^2}+n\frac{\partial^2 \Theta}{\partial z^2}\right),\\
&\frac{\partial \Theta}{\partial t}+Pe\frac{\partial \Theta}{\partial x}-V=\nabla^2\Theta,\\
&y=0: \qquad V=0, \quad \frac{\partial \Theta}{\partial y}=-1,\\
&y=1: \qquad \frac{\partial V}{\partial y}=0, \quad \Theta=0.
\end{aligned} \tag{12}$$

We assume solutions of Eq. (12) having the form of normal modes,

$$\begin{aligned}
V(x,y,z,t)&=f(y)e^{\eta\, t}e^{i(\alpha_x x+\alpha_z z-\omega t)},\\
\Theta(x,y,z,t)&=h(y)e^{\eta\, t}e^{i(\alpha_x x+\alpha_z z-\omega t)},
\end{aligned} \tag{13}$$

where η is the growth/decay rate, $\boldsymbol{\alpha}=(\alpha_x, 0, \alpha_z)$ is the wave vector and ω is the angular frequency. The parameters $(\alpha_x, \alpha_z, \eta, \omega)$ are real while (f, h) are, in general, complex functions. The growth rate η marks the difference between stability $(\eta<0)$ and instability $(\eta>0)$. The neutrally stable configuration is identified with $\eta=0$. The condition of minimum $\tilde{R}$ among the neutrally stable modes defines the critical values α_{cr} and $\tilde{R}_{cr}$.

By substituting definitions (13) into Eq. (12), one obtains the eigenvalue problem for neutrally stable modes,

$$\begin{aligned}
&f''-\frac{\alpha^2+(n-1)\alpha_z^2}{n}(f-\tilde{R}\,h)=0,\\
&h''-\left(\alpha^2-i\,\tilde{\omega}\right)h+f=0,\\
&y=0: \qquad f=0, \quad h'=0,\\
&y=1: \qquad f'=0, \quad h=0,
\end{aligned} \tag{14}$$

where $\alpha=(\alpha_x^2+\alpha_z^2)^{1/2}$ is the wave number of the disturbances. Moreover, the parameters $\tilde{R}$ and $\tilde{\omega}$ are defined as

$$\tilde{R}=\frac{R}{Pe^{n-1}}, \qquad \tilde{\omega}=\omega-\alpha_x Pe. \tag{15}$$

By denoting with ϕ the inclination angle of the wave vector $\boldsymbol{\alpha} = (\alpha_x, 0, \alpha_z)$ to the x axis, one obtains $\alpha_x = \alpha\cos\phi$ and $\alpha_z = \alpha\sin\phi$. The inclination angle $\phi = 0$ defines the transverse rolls while $\phi = \pi/2$ defines the longitudinal rolls. One may introduce a modified power–law index $\tilde{n}$ given by

$$\tilde{n} = \frac{n}{1 + (n-1)\sin^2\phi}. \tag{16}$$

The governing equations (14) can now be simplified as

$$f'' - \frac{\alpha^2}{\tilde{n}}(f - \tilde{R}\,h) = 0, \tag{17a}$$

$$h'' - \left(\alpha^2 - i\,\tilde{\omega}\right) h + f = 0, \tag{17b}$$

$$\begin{aligned} y = 0: &\qquad f = 0, \quad h' = 0, \\ y = 1: &\qquad f' = 0, \quad h = 0. \end{aligned} \tag{17c}$$

3.1. A proof that the stability eigenvalue problem is self–adjoint

We aim to prove that $\tilde{\omega} = 0$ and thus that the eigenvalue problem (17) is self–adjoint, namely that the eigenfunctions (f, h) are real–valued. On multiplying Eq. (17a) by the complex conjugate of function f and integrating by parts over the domain $[0, 1]$, one obtains

$$\int_0^1 |f'|^2 dy + \frac{\alpha^2}{\tilde{n}}\int_0^1 |f|^2 dy - \frac{\alpha^2\tilde{R}}{\tilde{n}}\int_0^1 f^* h\,\mathrm{d}y = 0, \tag{18}$$

where the complex conjugate is denoted by a star. Since $(\alpha, \tilde{R}, \tilde{n})$ are real parameters, Eq. (18) yields

$$\int_0^1 f^* h\,\mathrm{d}y \in \Re, \tag{19}$$

so that one obtains

$$\int_0^1 h^* f\,\mathrm{d}y \in \Re. \tag{20}$$

On multiplying Eq. (17b) by the complex conjugate of function h and integrating by parts one obtains

$$\int_0^1 |h'|^2\,\mathrm{d}y + (\alpha^2 - i\tilde{\omega})\int_0^1 |h|^2\,\mathrm{d}y - \int_0^1 h^* f\,\mathrm{d}y = 0. \tag{21}$$

By taking the imaginary part of Eq. (21), one may conclude that

$$\tilde{\omega}\int_0^1 |h|^2\,\mathrm{d}y = 0. \tag{22}$$

Equation (22) may be satisfied when either $h = 0$ or $\tilde{\omega} = 0$. The first option can be excluded since it yields the trivial solution $f = h = 0$. Thus we have proved that $\tilde{\omega} = 0$. This conclusion, together with Eq. (15), yields $\omega = \alpha_x\,Pe = \alpha\,Pe\cos\phi$. In other words, the transverse rolls travel at the same velocity as the basic flow, while the longitudinal rolls are non–travelling.

4. Solution techniques

The eigenvalue problem (17) involves two ordinary differential equations at constant coefficients. Therefore, it can be solved analytically by the elementary method of the characteristic equation. Then, the constraint that the solution be non–trivial yields a dispersion relation linking implicitly $\tilde{R}$ to α and $\tilde{n}$. This

	$\tilde{R}_c$		α_c	
$\tilde{n}$	Hybrid	Numerical	Hybrid	Numerical
0.1	7.09731575835505	7.09731575835494	1.07387719502812	1.07387719502818
0.2	8.91340448172414	8.91340448172405	1.22085343036798	1.22085343036801
0.3	10.3596927079765	10.3596927079764	1.32569911277239	1.32569911277227
0.4	11.6242074657406	11.6242074657404	1.41041580820013	1.41041580820012
0.5	12.7757161614035	12.7757161614034	1.48272234233180	1.48272234233181
0.6	13.8482400250468	13.8482400250467	1.54644147613404	1.54644147613405
0.7	14.8614997771314	14.8614997771314	1.60379713170813	1.60379713170815
0.8	15.8281205764997	15.8281205764996	1.65621450328595	1.65621450328596
0.9	16.7567581741586	16.7567581741586	1.70466901727952	1.70466901727953
1.	17.6536526097729	17.6536526097728	1.74986116307449	1.74986116307451
1.1	18.5234787451774	18.5234787451773	1.79231289340109	1.79231289340111
1.2	19.3698469531193	19.3698469531192	1.83242468865091	1.83242468865093
1.3	20.1956150748759	20.1956150748759	1.87051124793934	1.87051124793936
1.4	21.0030918653443	21.0030918653443	1.90682481943564	1.90682481943566
1.5	21.7941747467272	21.7941747467271	1.94157101406833	1.94157101406834
1.6	22.5704460614859	22.5704460614858	1.97491985509503	1.97491985509505
1.7	23.3332421492141	23.3332421492141	2.00701370114979	2.00701370114981
1.8	24.0837040741284	24.0837040741283	2.03797305559185	2.03797305559187
1.9	24.8228156306884	24.8228156306883	2.06790090969595	2.06790090969598
2.	25.5514323228069	25.5514323228068	2.09688604575922	2.09688604575925

Table 1: $\tilde{R}_c$ and α_c obtained for different values of $\tilde{n}$ and by means of two different solution techniques: hybrid analytical/numerical and fully numerical

analytical dispersion relation is rather complicated thus, for the sake of brevity, we do not report it here. A numerical root–finding algorithm can be employed to detect the numerical value of $\tilde{R}$ for any given pair $(\alpha, \tilde{n})$. This allows one to draw the neutral stability curves $\tilde{R}(\alpha)$ for different values of $\tilde{n}$. This, then, is the hybrid analytical/numerical approach to the solution of Eq. (17). We mention here that the root–finding algorithm is based on the Newton–Raphson method.

The second approach is entirely numerical. We transform the eigenvalue problem (17) into an initial value problem by completing the initial conditions set at $y = 0$,

$$\begin{aligned} & f'' - \frac{\alpha^2}{\tilde{n}}(f - \tilde{R}\, h) = 0, \\ & h'' - \alpha^2 h + f = 0, \\ & y = 0: \qquad f = 0, \quad f' = \xi, \quad h = 1, \quad h' = 0, \end{aligned} \tag{23}$$

where ξ is an unknown real parameter the scale–fixing condition $h = 1$ can be imposed because the system (17) is homogeneous. The Runge–Kutta method is employed to solve the initial value problem (23). The eigenfunctions depend on the parameters $(\alpha, \tilde{n}, \tilde{R}, \xi)$. Then, the shooting method is employed to obtain, for given $(\alpha, \tilde{n})$, the pair $(\tilde{R}, \xi)$ using the target conditions $f' = 0$ and $h = 0$ at $y = 1$. Again, a root–finding algorithm serves to evaluate $\tilde{R}$ and ξ.

These solution methods are compared in Table 1. In this table, the critical values of $\tilde{R}$ and α are reported for given $\tilde{n}$. The results presented are obtained by employing 15 digits of precision. Table 1 allows one to conclude that the two different methods yield, within at least 13 significant figures, the same results. Since the hybrid analytical/numerical method displays a better performance, namely a shorter computational time and the ability to explore very small values of $\tilde{n}$, any further results presented here are obtained by this method.

The neutral stability curves $\tilde{R}(\alpha)$ are reported in Fig. 2. These curves move upward and rightward

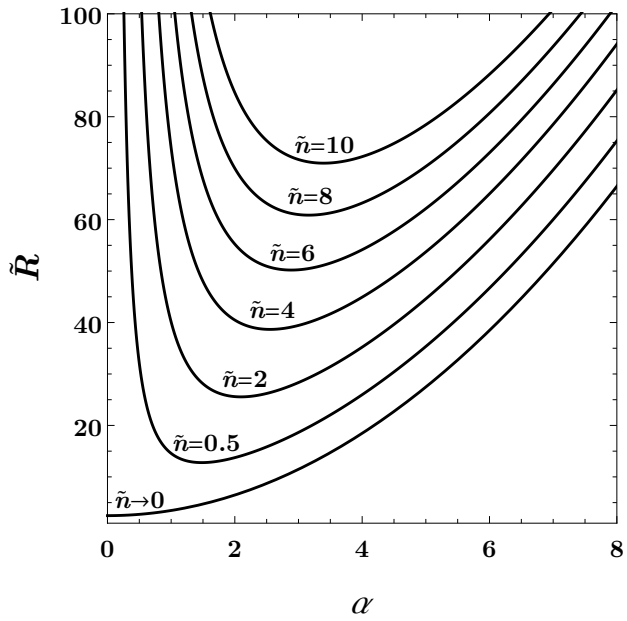

Figure 2: Neutral stability curves $\tilde{R}(\alpha)$ for fixed values of $\tilde{n}$

monotonically with increasing values of the parameter $\tilde{n}$. This behaviour can be found again in Fig. 3 where the critical values of $\tilde{R}$ and α are plotted versus $\tilde{n}$. The limiting case $\tilde{n} \to 0$ deserves some particular attention.

4.1. Asymptotic solution for $\tilde{n} \to 0$

When the parameter $\tilde{n} \to 0$, the eigenvalue problem (17) degenerates into a second differential problem,

$$h'' - (\alpha^2 - \tilde{R})h = 0, \qquad h'(0) = 0, \qquad h(1) = 0. \tag{24}$$

The solution of the differential equation (24) satisfying the initial condition $h'(0) = 0$ is, up to an arbitrary multiplicative constant,

$$h = \cosh\left(y\sqrt{\alpha^2 - \tilde{R}}\right). \tag{25}$$

By imposing the boundary condition $h'(1) = 0$, one obtains an expression for $\tilde{R}$, namely

$$\tilde{R} = \alpha^2 + \frac{\pi^2}{4}(2\,m + 1)^2, \qquad m = 0, 1, 2, \ldots \tag{26}$$

With $m = 0$, one obtains the neutral stability curve for $\tilde{n} \to 0$ presented in Fig. 2. Moreover, one may evaluate the critical values $\tilde{R}_c = \pi^2/4$ and $\alpha_c = 0$.

5. Results

A easier interpretation of the results is drawn when they are expressed in terms of the parameters n and R. Equation (15) allows one to conclude that, for given values of n and Pe, the value of R_c is immediately obtained from the value of $\tilde{R}_c$. From Fig. 3, one infers that $\tilde{R}_c$ is a monotonic increasing function of $\tilde{n}$. Moreover, Eq. (16) implies that $\tilde{n}$ is a monotonic increasing function of ϕ when $n < 1$ while it is a monotonic decreasing function of ϕ when $n > 1$. Thus, our conclusion is that, the most unstable condition is attained

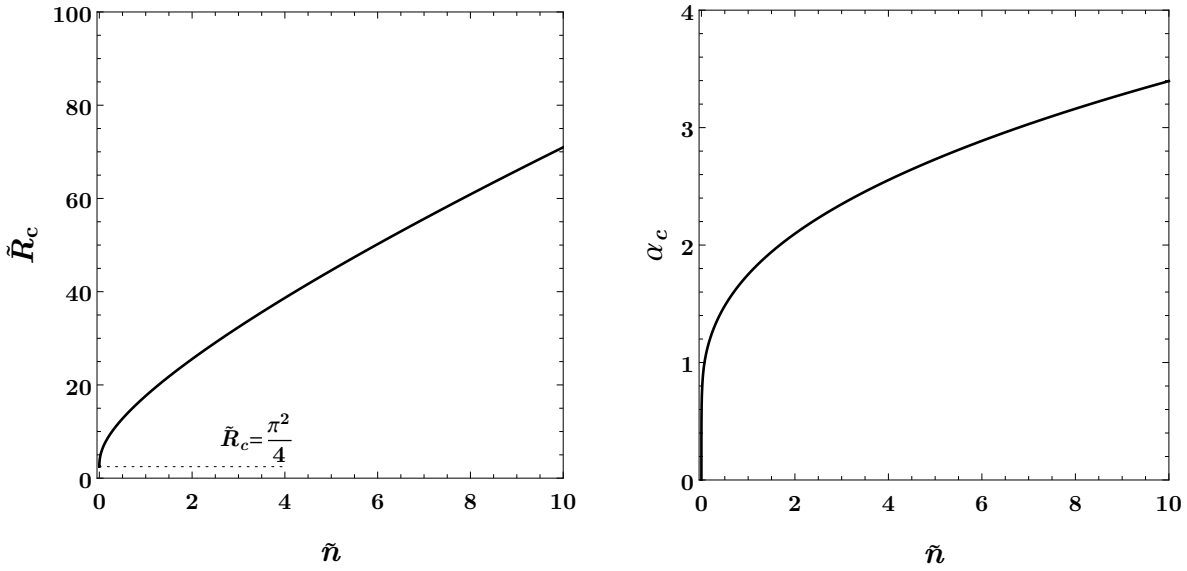

Figure 3: Critical values of $\tilde{R}$ and α versus $\tilde{n}$

with transverse rolls ($\phi = 0$) for $n < 1$, and with longitudinal rolls ($\phi = \pi/2$) for $n > 1$. Just the same conclusion has been reported in [7].
For $n < 1$, we consider transverse rolls which yield $\tilde{n} = n$ and thus

$$n < 1 \qquad \longrightarrow \qquad R_c = \tilde{R}_c(n)\, Pe^{n-1}, \qquad \alpha_c = \alpha_c(n). \tag{27}$$

In the limiting case $n \to 0$, we obtained $\tilde{R}_c = \pi^2/4$ so that Eq. (27) yields $R_c = \pi^2/(4\, Pe)$.
For a Newtonian fluid, one obtains $\tilde{n} = 1$ and thus, on account of the data reported in Table 1, one has

$$n = 1 \qquad \longrightarrow \qquad R_c = 17.653653, \qquad \alpha_c = 1.7498612. \tag{28}$$

It is worth noting for Newtonian fluids R_c and α_c are independent of ϕ. The critical values in Eq. (28) agree with those reported in Table 6.1 of Nield and Bejan [1] for the same boundary conditions.
For $n > 1$, we consider longitudinal rolls which yield $\tilde{n} = 1$ and thus

$$n > 1 \qquad \longrightarrow \qquad R_c = 17.653653\, Pe^{n-1}, \qquad \alpha_c = 1.7498612. \tag{29}$$

The results reported in Eqs. (27)–(29) are presented in Fig. 4. The critical values of the modified Darcy–Rayleigh number are reported versus the power–law index n for different values of the Péclet number. From Fig. 4, one may conclude that the Péclet number has a destabilising effect for pseudoplastic fluids while it has a stabilising effect for dilatant fluids. On the other hand, the power–law index n has a stabilising effect for the basic state when $Pe \geqslant 0.60653066$ while, when $Pe < 0.60653066$, n has a non monotonic effect on the value of R_c.

6. Conclusions

The basic horizontal throughflow across a fluid saturated porous layer, parametrised by the Péclet number Pe, has been studied with a special focus on buoyancy–induced thermal convection. The saturating fluid is non–Newtonian, described by a power–law model. The lower boundary of the layer is uniformly heated and impermeable, while the upper boundary is assumed to be open and isothermal. The basic state is

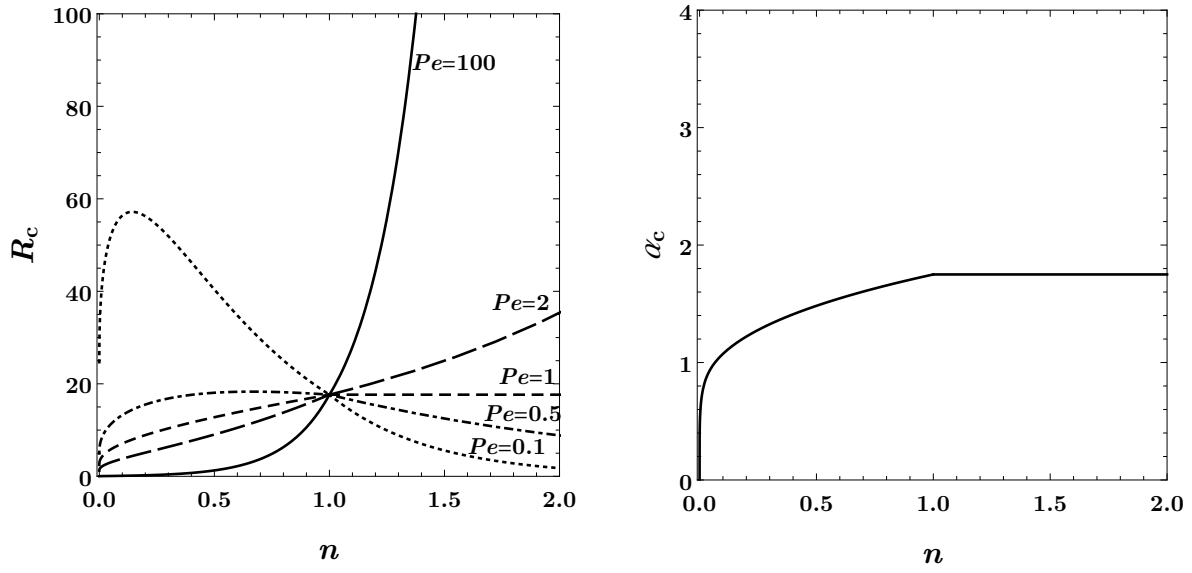

Figure 4: Critical values of R and α versus the power–law index n for fixed values of Pe

perturbed by means of plane wave disturbances inclined arbitrarily to the direction of the basic flow. The linear stability analysis of such disturbances is carried out by employing two different techniques: a hybrid analytical/numerical method and a fully numerical method. The critical values of the governing parameters, the modified Darcy–Rayleigh number R and the wavenumber α, are obtained. The main results are the following:

- When a Newtonian fluid is considered, the critical values of the modified Darcy–Rayleigh number and of the wavenumber match those reported in the literature [1]: $R_c = 17.653653$ and $\alpha_c = 1.7498612$.
- For pseudoplastic fluids, the transverse rolls are the most unstable modes while, for dilatant fluids, the most unstable disturbances are the longitudinal rolls.
- The longitudinal rolls are non–travelling plane waves while the transverse rolls travel with the same dimensionless velocity as the basic flow.
- For the limiting case of a vanishingly small power–law index, the critical values are obtained analytically: $R_c = \pi^2/(4\,Pe)$ and $\alpha_c = 0$.
- An increasing power–law index has a stabilising effect for the basic state with $Pe > 0.60653066$, while it has a non–monotonic effect for $Pe \geqslant 0.60653066$.
- The Péclet number is a destabilising parameter for pseudoplastic fluids, while it is a stabilising parameter for dilatant fluids.
- The critical value of the wavenumber independent of Pe. This value is a monotonic increasing function of the power–law index for pseudoplastic fluids, while it is constant for dilatant fluids.

Declaration of competing interest

The authors declare that they have no known competing financial interests or personal relationships that could have appeared to influence the work reported in this paper.

Acknowledgment

The authors acknowledge the financial support from the grant PRIN 2017F7KZWS provided by the Italian Ministry of Education and Scientific Research.

References

[1] D. Nield, A. Bejan, Convection in Porous Media, 5th ed., Springer, New York, 2017.

[2] C. Horton, F. Rogers, Convection currents in a porous medium, Journal of Applied Physics 16 (1945) 367–370.

[3] E. Lapwood, Convection of a fluid in a porous medium, Mathematical Proceedings of the Cambridge Philosophical Society 44 (1948) 508–521.

[4] M. Prats, The effect of horizontal fluid flow on thermally induced convection currents in porous mediums, Journal of Geophysical Research 71 (1966) 4835–4838.

[5] R. Chhabra, J. Richardson, Non–Newtonian flow and applied rheology, in: Non–Newtonian Flow and Applied Rheology, second edition ed., Butterworth-Heinemann, Oxford, 2008, pp. 1–55.

[6] A. Shenoy, Non–Newtonian fluid heat transfer in porous media, in: Advances in Heat transfer, volume 24, Elsevier, 1994, pp. 101–190.

[7] A. Barletta, D. Nield, Linear instability of the horizontal throughflow in a plane porous layer saturated by a power-law fluid, Physics of Fluids 23 (2011) 013102.

[8] M. Celli, A. Barletta, S. Longo, L. Chiapponi, V. Ciriello, V. Di Federico, A. Valiani, Thermal instability of a power–law fluid flowing in a horizontal porous layer with an open boundary: A two–dimensional analysis, Transport in Porous Media (2017) 1–23.

[9] A. Nakayama, A. Shenoy, Combined forced and free convection heat transfer in power–law fluid–saturated porous media, Applied Scientific Research 50 (1993) 83–95.

[10] A. Shenoy, Darcy–Forchheimer natural, forced and mixed convection heat transfer in non-Newtonian power–law fluid–saturated porous media, Transport in Porous Media 11 (1993) 219–241.

[11] R. H. Christopher, S. Middleman, Power–law flow through a packed tube, Industrial & Engineering Chemistry Fundamentals 4 (1965) 422–426.

[12] A. Shenoy, Heat Transfer to Non–Newtonian Fluids: Fundamentals and Analytical Expressions, John Wiley & Sons, 2018.